Microwave response of thin niobium films under perpendicular static magnetic fields

Janjušević, Dragan; Grbić, Mihael Srđan; Požek, Miroslav; Dulčić, Antonije; Paar, Dalibor; Nebendahl, Bernd; Wagner, Thomas

Source / Izvornik: **Physical review B: Condensed matter and materials physics, 2006, 74**

Journal article, Published version
Rad u časopisu, Objavljena verzija rada (izdavačev PDF)

https://doi.org/10.1103/PhysRevB.74.104501

Permanent link / Trajna poveznica: https://urn.nsk.hr/urn:nbn:hr:217:920247

Microwave response of thin niobium films under perpendicular static magnetic fields

D. Janjušević, M. S. Grbić, M. Požek,* A. Dulčić, and D. Paar
Department of Physics, Faculty of Science, University of Zagreb, P. O. Box 331, HR-10002 Zagreb, Croatia

B. Nebendahl†
Physikalisches Institut, Universität Stuttgart, D-70550 Stuttgart, Germany

T. Wagner
Max-Planck-Institute for Metals Research, Heisenbergstrasse 3, D-70156 Stuttgart, Germany
(Received 7 February 2006; revised manuscript received 4 May 2006; published 1 September 2006)

The microwave response of high quality niobium films in a perpendicular static magnetic field has been investigated. The complex frequency shift was measured up to the upper critical fields. The data have been analyzed by the effective conductivity model for the type-II superconductors in the mixed state. This model is found to yield consistent results for the coherence lengths in high-κ superconducting samples, and can be used with high-temperature superconductors even at temperatures much below T_c. It is shown that for samples with high values of depinning frequency, one should measure both components of the complex frequency shift in order to determine the flow resistivity. The thick Nb film (160 nm) has low resistivity at 10 K, comparable to the best single crystals, and low κ value. In contrast, the thinnest (10 nm) film has $\kappa \approx 9.5$ and exhibits a high depinning frequency ($\approx$20 GHz). The upper critical field determined from microwave measurements is related to the radius of nonoverlaping vortices, and appears to be larger than the one determined by the transition to the normal state.

DOI: 10.1103/PhysRevB.74.104501 PACS number(s): 74.78.Db, 74.25.Nf, 74.25.Op, 74.25.Qt

I. INTRODUCTION

Microwave investigations of classical superconductors half a century ago have proven to be a very useful tool in the determination of intrinsic parameters in the Meissner state[1–3] as well as the flow resistivity in the mixed state.[4–6] These investigations were also of large technical interest for the construction of microwave transmission lines and resonant structures. In the last twenty years high-temperature superconductors (HTSCs) have been extensively investigated by microwave techniques. Among the greatest successes, one should mention the determination of the temperature dependence of the penetration depth which evidenced the existence of nodes in the superconducting gap, leading to the *d*-wave explanation of HTSCs.[7]

Flux flow resistivity can be determined from dc measurements when the current density J exceeds the critical current density J_c for vortex depinning.[8] However, in many cases of low- and high-temperature superconductors, the dynamics of vortex motion is more complicated and cannot be interpreted just in terms of pinned and depinned regimes. Thermally activated flux hopping may yield Ohmic behavior even for current densities below J_c.[9] However, the resistivity observed in this regime should not be identified with that of flux flow. By increasing the current density there occurs a nonlinear transition to the flux flow regime. At much higher current densities one may encounter nonlinear effects in the flux flow leading ultimately to the point of instability where a dramatic increase of the measured voltage occurs.[10–15] The nonlinear behavior is temperature and magnetic-field dependent. Hence the linear flux flow regime may occur in between the two nonlinear regimes, and may not always be well resolved.

In contrast to dc resistivity, microwave measurements can be carried out with current densities much smaller than J_c, and still yield flux flow resistivity. Namely, the vortices are not driven over the pinning potential barrier, but just oscillate within the potential well.

Depinning frequency ω_0 separates two regimes of vortex oscillation. If the driving frequency ω is much larger than ω_0, the viscous drag force dominates over the restoring pinning force in the response of vortices to the microwave Lorentz force. This is often the case with classical superconductors which have ω_0 in the MHz range. In that case, the flux flow resistivity can be extracted from the microwave absorption curves only. When $\omega_0 \approx \omega$, or higher, the restoring pinning force is comparable to the viscous drag force, and the response of the vortices is more complex. This is typical of HTSCs where the depinning frequency is found to be of the order of 10 GHz,[16] but may be found also in low-temperature superconductors such as in very thin Nb film analyzed in this paper below. In such cases, one needs both microwave absorption and dispersion to determine the depinning frequency and flux flow parameters. The analysis usually employs the models of effective conductivity in the mixed state[17–19] based on the Bardeen-Stephen model.[20]

The real values of B_{c2} in HTSCs remain experimentally unreachable except for the narrow temperature range below T_c, and the B_{c2} values extracted from the effective conductivity data could not be experimentally verified. In order to probe the effective conductivity model, we have performed a series of measurements on thin films and a single crystal of niobium, a classical type-II superconductor. The comparison of thick niobium samples with HTSC samples is not ideal since the upper critical fields and depinning frequencies in niobium are much lower and the vortex distance does not always allow the use of effective conductivity models. However, as the film thickness is reduced, one expects considerable enhancement of B_{c2}, due to the reduced coherence

length, and much stronger pinning, due to the surface effects.

We have measured high quality niobium thin films using a cavity perturbation method. The temperature and field dependence of the complex frequency shift have been measured up to the upper critical fields in order to test the validity of the effective conductivity models. The results of the present analysis should be taken into account when the mixed state of HTSCs is investigated by the microwave methods.

II. SAMPLES

The Nb films were deposited via molecular beam epitaxy (MBE) in a commercial system from DCA instruments (Finland). The base pressure of the system is 10^{-9} Pa. The (0001) surfaces of the sapphire substrates (α-Al_2O_3) were prepared by sputter cleaning with Ar ions (1 keV) and subsequent annealing at 1000 °C in ultrahigh vacuum (UHV). This annealing procedure is necessary to remove the embedded Ar gas atoms and to recover the sapphire surface crystallography and morphology. Details of the surface preparation procedure can be found elsewhere.[21–23] The substrate treatment resulted in unreconstructed surfaces, as revealed by reflection high-energy electron diffraction (RHEED). Niobium (4 N purity) was evaporated from an electron beam evaporator (substrate temperature 900 °C; film thicknesses 10, 40, 160 nm) and the growth rate was monitored using a quartz oscillator. Typical growth rates were between 0.01 and 0.05 nm/s. As revealed by *in situ* RHEED investigations, the Nb films grew epitaxially on the (0001) sapphire substrate.[23] A 2-nm-thick protective layer of SiO_2 has been deposited onto each film in order to prevent niobium oxidation (physical vapor deposition at room temperature). Transmission electron microscopy (TEM) investigations have shown that the film of nominal thickness 40 nm is actually 36 nm thick, indicating that the other films are also slightly thinner than their nominal thickness. The samples were cut by a diamond saw into pieces 3×0.5 mm^2 (40 and 160 nm films), and 2.3×1 mm^2 (10-nm film), suitable for cavity perturbation measurements. A high-purity single crystal of niobium was purchased from Metal Crystals & Oxides Ltd., Cambridge. Its dimensions were $3\times2\times0.5$ mm^3.

Superconducting properties of thin niobium films strongly depend on their thickness, purity, and preparation conditions.[24–29] In order to compare our samples with those measured earlier,[24–26] we have determined the T_c of each film by the so-called 90% criterion, i.e., the transition temperature was defined as the temperature where microwave absorption $\Delta(1/2Q)$ reaches 90% of its normal-state value. For the samples of the same composition and purity one expects that T_c is reduced approximately with the inverse thickness d^{-1} due to the proximity effects,[30] weak localization, and increased residual resistivity.[26] We show in Fig. 1 the comparison of transition temperatures of our thin films with results of some other authors. The T_c values of present films are similar to the films measured by Gubin *et al.*,[28] and, if extrapolated to ultrathin 2 nm, with the film measured by Hsu and Kapitulnik.[29] Obviously, the films measured in this paper are of good quality.

To extract various superconducting parameters one needs three quantities: T_c, ρ_n, and $S=-dB_{c2}/dT$ at T_c. The B_{c2} values determined also by the 90% criterion from our measurements gave the S values 0.47, 0.11, and 0.08 T/K for 10-, 40-, and 160-nm samples, respectively.

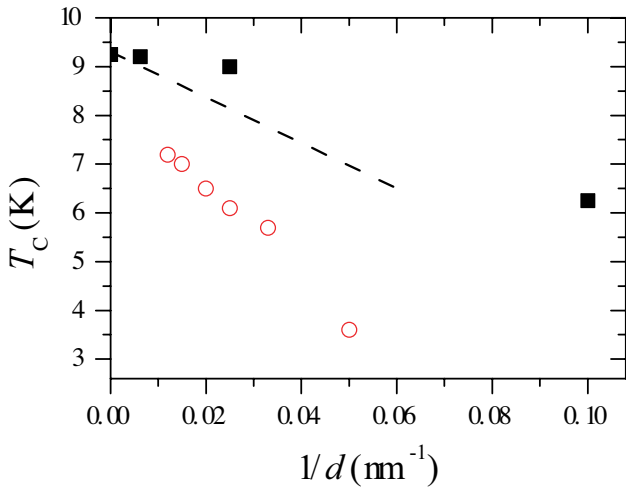

FIG. 1. (Color online) Thickness dependence of the transition temperature of the measured niobium films (full squares). The data are compared with clean samples of Wolf *et al.* (Ref. 24) and Kodama *et al.* (Ref. 25) (dashed line), and with dirty samples of Minhaj *et al.* (Ref. 26) (circles).

The resistivities of the films have been determined by standard four contact method. Their residual values at $T=10$ K were $\rho_n(10\text{ nm})=15.2\ \mu\Omega$ cm, $\rho_n(40\text{ nm})=1.4\ \mu\Omega$ cm and $\rho_n(160\text{ nm})=0.33\ \mu\Omega$ cm, respectively. The residual resistivity of the 160-nm film was found to be an order of magnitude lower than in the film studied by Gubin *et al.*,[28] and comparable to the best bulk single crystals,[3,31] showing that the films grew with perfect epitaxy with virtually no defects. The residual resistivities of thinner samples are therefore increased only due to the surface scattering, but the values are still below the values reported by Gubin *et al.*[28] For the 10-nm film we estimate $\kappa\approx9.5$, for the 40-nm film $\kappa\approx1.5$, and for the 160-nm film we can take the single crystal value of $\kappa\approx0.9$.

III. EXPERIMENTAL DETAILS

Microwave measurements were carried out in a high-Q elliptical cavity made of copper resonating in ${}_e\text{TE}_{111}$ mode at 9.3 GHz or in ${}_e\text{TE}_{113}$ mode at 17.5 GHz. For both modes used, the microwave magnetic field has a node in the center of the cavity while the microwave electric field is at maximum. The sample was mounted on a sapphire sample holder and placed in the center of the cavity where the microwave electric field E_{mw} has its maximum in both modes. The sample was oriented with the longest side parallel to $\boldsymbol{E}_{mw}$. The experimental setup included an Oxford Systems superconducting magnet with $\boldsymbol{B}_{dc}\perp\boldsymbol{E}_{mw}$. While $\boldsymbol{E}_{mw}$ is always in the film plane, $\boldsymbol{B}_{dc}$ can be in the film plane or perpendicular to it. Directly measured quantities are the Q factor and the resonant frequency f of the cavity loaded with the sample. The Q factor was measured by a modulation technique described elsewhere.[32] The empty cavity absorption $(1/2Q)$

was substracted from the measured data and the presented experimental curves are due to the samples themselves. An automatic frequency control (AFC) system was used to set the source frequency always in resonance with the cavity. Thus the frequency shift can be measured as the temperature of the sample or static magnetic field is varied. The two measured quantities represent the complex frequency shift $\Delta\tilde{\omega}/\omega=\Delta f/f+i\Delta(1/2Q)$.

IV. EFFECTIVE CONDUCTIVITY

For the extraction of complex conductivity data from the measured complex frequency shift of a thin superconducting sample in the microwave electric field, one can utilize the general solution for the complex frequency shift by Peligrad *et al.*[33] The shift from a perfect conductor state is given by

$$\frac{\Delta\tilde{\omega}_p}{\omega}=\frac{\Gamma}{N}\left[1+\left(\frac{\tilde{k}^2}{k_0^2}\frac{\tanh(i\tilde{k}d/2)}{i\tilde{k}d/2}-1\right)N\right]^{-1}, \quad (1)$$

where d is the thickness of the slab, N is the depolarization factor, and Γ is the dimensionless filling factor of the sample in the cavity. The complex wave vector $\tilde{k}$ is given by

$$\tilde{k}=k_0\sqrt{\tilde{\mu}_r\left(\tilde{\epsilon}_r-i\frac{\tilde{\sigma}}{\epsilon_0\omega}\right)}, \quad (2)$$

where $k_0=\omega\sqrt{\mu_0\epsilon_0}$ is the vacuum wave vector. It describes generally any set of material parameters. For a nonmagnetic metal one can take $\tilde{\mu}_r=\tilde{\epsilon}_r=1$ and the main contribution to $\tilde{k}$ comes from conductivity. Using these equations one can by numerical inversion of experimentally obtained complex frequency shift determine the complex conductivity $\tilde{\sigma}$ of the sample.

For a superconducting sample in the mixed state, in intermediate fields one can define the effective complex conductivity[17–19] which is a combination of normal conductivity in the vortex cores and the conductivity of the condensed electrons outside the cores. The effective conductivity in an oscillating electric field is given by

$$\frac{1}{\tilde{\sigma}_{\text{eff}}}=\frac{1-b/[1-i(\omega_0/\omega)]}{(1-b)(\sigma_1-i\sigma_2)+b\sigma_n}+\frac{1}{\sigma_n}\frac{b}{1-i(\omega_0/\omega)}. \quad (3)$$

The first term is due to the microwave current outside the vortex cores, and the second is due to the normal current in the cores of the oscillating vortices. The meaning of the parameter b in Eq. (3) is the volume fraction of the sample taken by the normal vortex cores. This parameter determines the resistivity in the flux flow regime ρ_f/ρ_n.[34] The depinning frequency ω_0 may vary, depending on sample, field, and temperature from the strongly pinned case ($\omega_0\gg\omega$) to the flux flow limit ($\omega_0\ll\omega$). In Eq. (3) the zero-field conductivity is $\sigma_1-i\sigma_2$, and σ_n is the normal-state conductivity. The model is limited to high κ values and to magnetic fields much lower than upper critical fields, where vortices do not overlap significantly.

From the experimentally obtained field-dependent complex conductivity extracted using Eqs. (1) and (2) one can, by numerical inversion of Eq. (3), determine the values of b and ω_0/ω.

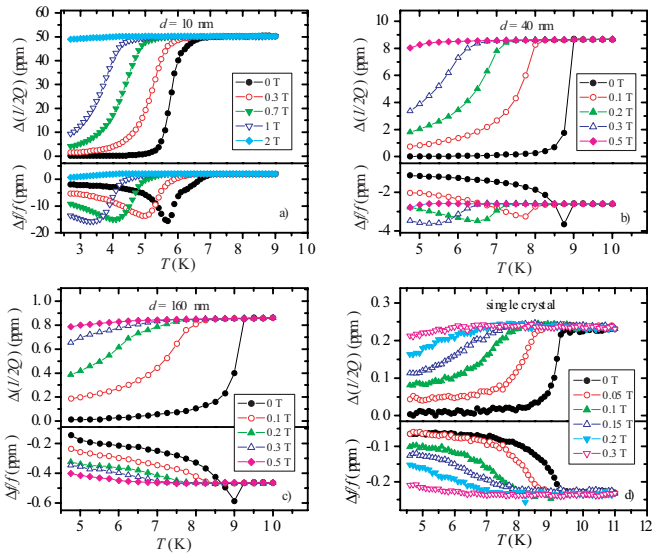

FIG. 2. (Color online) Measured temperature dependence of complex frequency shift of four niobium samples: (a) thin film $d=10$ nm; (b) thin film $d=40$ nm; (c) thin film $d=160$ nm; (d) single crystal. The driving frequency was 9.3 GHz. Applied perpendicular static magnetic fields are indicated in the legends.

V. RESULTS AND DISCUSSION

The measured complex frequency shift of the three films and the single crystal is presented in Fig. 2 for various values of dc magnetic field and for a driving frequency 9.3 GHz. One may notice a huge difference in signal intensities between thin and thick samples due to very different filling factors Γ. Namely, a conducting sample profoundly changes the electric field at the center of the cavity with respect to the empty cavity field. The sample acts as a partial short for the electric-field lines.[35] The field outside of a conductor is stronger at the rear and front sides, and this enhancement is larger for thinner films. As a consequence, the microwave measurements in the electric field are very sensitive for thin films, while for thicker samples the signal-to-noise ratio is reduced.

Looking at the zero-field measurements in Fig. 2, one observes a smooth transition to the superconducting state for the thinnest film, and sharp transitions for thicker samples. In the 10-nm sample the fluctuation effects become considerable since the thickness becomes lower than the coherence length.

From the measured frequency shift and known normal-state resistivity ρ_n one can determine the complex conductivity in the whole temperature range and consequently the zero-temperature penetration depth. We have obtained $\lambda(T=0)=285$ nm for the 10-nm film, comparable to the result of Gubin *et al.*[28] for the film of the same thickness. The filling factor Γ was determined at $T=10$ K from the measured frequency shift and known normal-state resistivity for each

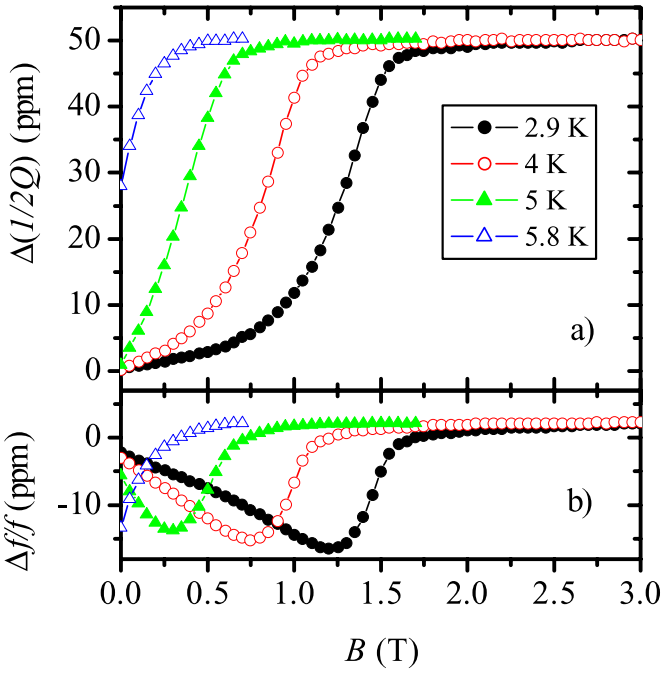

FIG. 3. (Color online) Field dependence of the complex frequency shift for the 10-nm film at various temperatures.

sample, and we keep it fixed in further analysis of a given sample.

Knowing the measured temperature dependence of the complex frequency shift in zero field, we are interested in its field dependence at fixed temperatures. As an example, we show the field dependence of the complex frequency shift for the 10-nm sample in Fig. 3. From these data one proceeds in two steps. First, the numerical inversion of complex frequency shift gives the field dependence of complex effective conductivity. Second, from this σ_{eff} one numerically determines[36] parameters b and ω_0 by the use of Eq. (3). The results are given in Fig. 4. One may notice that the depinning frequency is well above the driving frequency for the thinnest sample, contrary to the predictions $[\omega_0 \leq (2\pi)100\ \text{MHz}]$ for thick niobium samples.[6] We shall return to this point later.

The parameter b is shown in Fig. 4(a). In the effective conductivity model it is identified with the volume fraction of the normal cores of the vortices in the mixed state. The field dependence of this parameter has nearly linear region at lower fields, as expected for nonoverlapping vortices. It has a meaning of reduced field $b=B/B_{c2}^{*}$ in the model of Bardeen and Stephen,[20] where B_{c2}^{*} represents the hypothetical upper critical field given by the equation $B_{c2}^{*}=\Phi_0/[2\pi\xi(T)^2]$. Therefore from the linear section of its field dependence one can determine the radii of vortices and the Ginzburg-Landau (GL) coherence length at a given temperature. Detailed analysis of flow resistivity by Larkin and Ovchinnikov leads to the correction factor 0.9 for the linear regime, i.e., $b=0.9B/B_{c2}^{*}$.[37] The extrapolation of this linear section, shown by the dashed line in Fig. 4(a), would give $B_{c2}^{*}(2.9\ \text{K})=1.9$ T, and $\xi(2.9\ \text{K})=41$ nm. At higher fields b changes its slope and approaches the normal-state value at field B_{c2} lower than B_{c2}^{*}. It is the region where vortices start to overlap

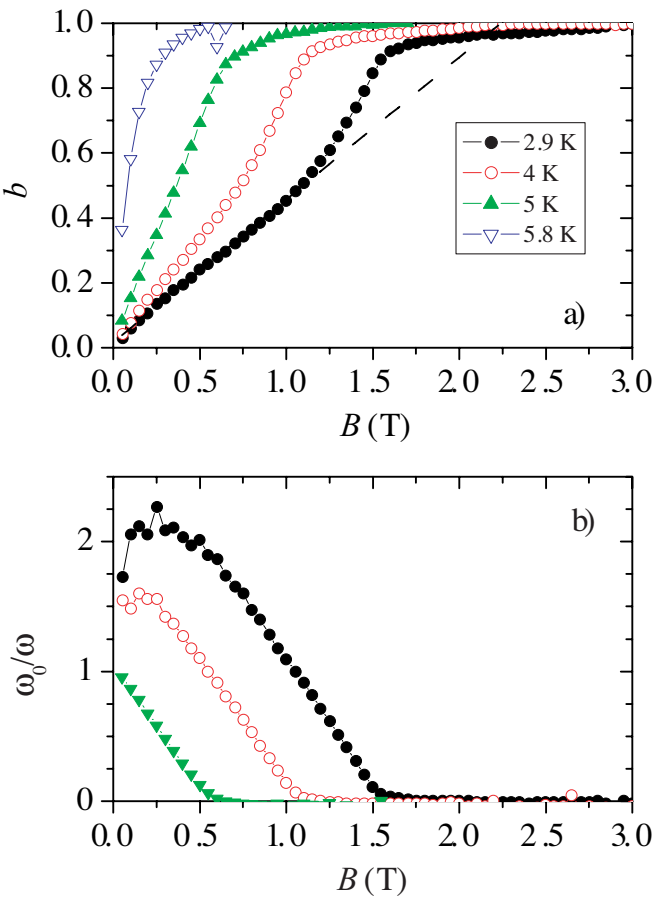

FIG. 4. (Color online) Parameters b and ω_0/ω of the effective conductivity model extracted from the data of Fig. 3. The dashed line shows the extrapolation of the linear section at $T=2.9$ K.

and the superconducting order parameter is reduced throughout the sample. The deviation from linearity starts roughly at the field $B=0.63\ B_{c2}$, where the distance between vortex centers is 3.4 times the coherence length.

One should mention that numerically determined b values do not always reach unity at B_{c2}. Close to B_{c2}, b loses its meaning as a parameter of the effective conductivity model. There are no more well defined vortices and the conductivity is dominated by fluctuations. One can still try to numerically obtain b and ω_0, but this leads to negative values of depinning frequencies, clearly showing the failure of the effective conductivity model in that region.

The determination of flow resistivity would not be possible if only the microwave absorption had been measured. The effective conductivity depends on two parameters (b and ω_0), and one has to measure two quantities, absorption and real frequency shift, in order to determine both parameters. If one supposed that the pinning at microwave frequencies were negligible, one could have determined the flow resistivity from absorption measurements alone. This would lead to wrong conclusions. We show in Fig. 5(a) the comparison of the two ways of reasoning for the 10-nm film at 2.9 K. The full circles show the parameter b determined from the complex frequency shift with the depinning frequency as the second result of the numerical inversion. The empty circles

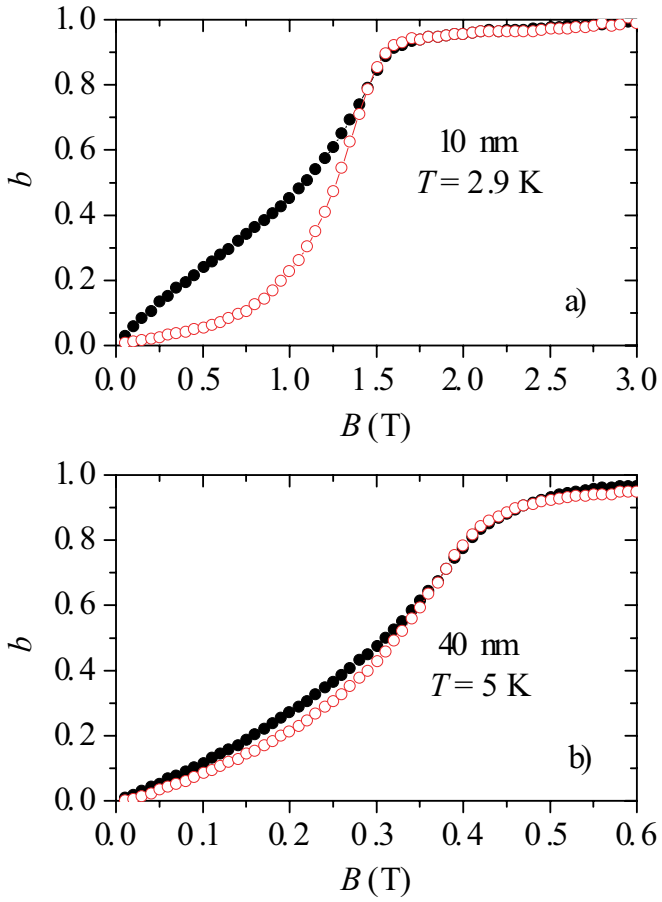

FIG. 5. (Color online) Comparison of b obtained by full inversion of complex frequency shift (full black circles) and b obtained from absorption measurement alone under the assumption that depinning frequency is much lower than driving frequency (red open circles): (a) 10-nm film at 2.9 K; (b) 40-nm film at 5 K.

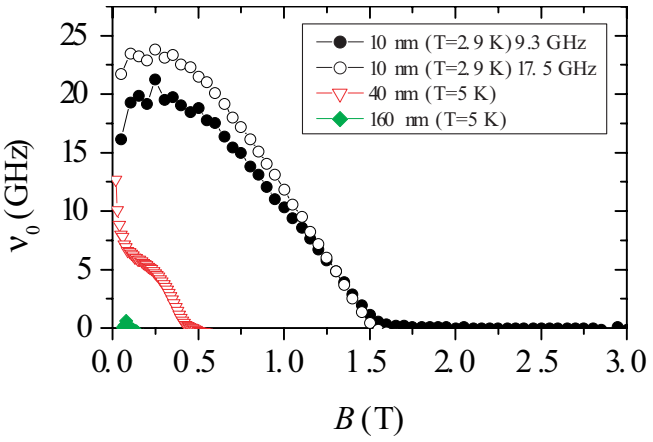

FIG. 6. (Color online) Field dependence of the depinning frequency $\nu_0=\omega_0/2\pi$ obtained by driving frequency 9.3 GHz for three niobium films at $T/T_c\approx 0.5$: 10 nm film at 2.9 K (black full circles); 40 nm film at 5 K (red opened triangles) and 160 nm film at 5 K (green full diamonds). The depinning frequency obtained by driving frequency 17.5 GHz for the 10 nm film at 2.9 K is shown by open black circles.

are the result of the numerical inversion of the microwave absorption only, under the assumption that $\omega_0=0$. One can see that the results differ strongly in the low-field region, i.e., in the region where the pinning is strong. When the depinning frequency falls well below the driving frequency, the two curves overlap. A similar analysis for the 40-nm sample is shown in Fig. 5(b). The two ways of reasoning give closer results since the depinning frequency for this sample is lower than the driving frequency ($\omega_0 \leq 0.7\omega$, see Fig. 6).

If one is dealing with the samples whose upper critical field is experimentally unreachable (as in HTSCs), one is led to infer the upper critical field from the slope of b in low fields. Taking the flow resistivity values from microwave absorption, without taking the real frequency shift into account, one could reach erroneous values of the upper critical field and GL coherence length. This is especially true for samples with high values of depinning frequency, which is usually the case in HTSCs.

Bulk metallic superconductors usually do not show pinning at microwave frequencies.[6] In Fig. 6 we show the depinning frequency of our three niobium films at $T\approx 0.5\ T_c$. The depinning frequency for the 10-nm film at low fields is slightly above 20 GHz, and for the 40-nm film it is approximately 7 GHz. For the 160-nm film it is below 1 GHz, i.e., in the frequency range that would be better examined by lower driving frequency. Obviously, in thin films placed in a perpendicular magnetic field, vortex pinning is dominated by surface pinning centers. Thicker films approach bulk values of depinning frequencies, showing that the presently grown niobium films do not have bulk pinning centers, which are absent also in the best single crystals.

To check the consistency of depinning frequency values obtained by different driving frequencies, we obtained the depinning frequency of the 10-nm sample from measurements in the ${}_eTE_{113}$ mode with driving frequency of 17.5 GHz. The result is shown by the open circles in Fig. 6, with satisfactory agreement between the two measurement series.

The above analysis for the 10-nm film clearly shows a linear section of b in moderate fields. Already for the 40-nm film, the linearity is not perfect. For the 160-nm film and for single crystal there were no linear sections. It is not surprising since the simple Bardeen-Stephen model predicts a linear dependence of ρ_f/ρ_n on B only in the high-κ limit. Obviously, only the thinnest film considered here fulfills the necessary conditions for the analysis in terms of the effective conductivity model. This result provides justification for the analysis of high-κ superconductor with high values of upper critical fields, typically HTSCs.

One can compare the values of B_{c2}, obtained by the 90% criterion, with the B_{c2}^* values obtained from the linear section of field dependence of b by taking into account the Larkin-Ovchinnikov correction $b=0.9B/B_{c2}^*$. The comparison is shown in Fig. 7. Full circles show B_{c2} obtained by the 90% criterion and opened circles show B_{c2}^* values obtained from linear section of b. One can see that B_{c2}^* is always slightly higher than B_{c2} which would be measured by direct transport or magnetization measurement of the crossover to the normal state, if experimentally reachable. The reduction of order pa-

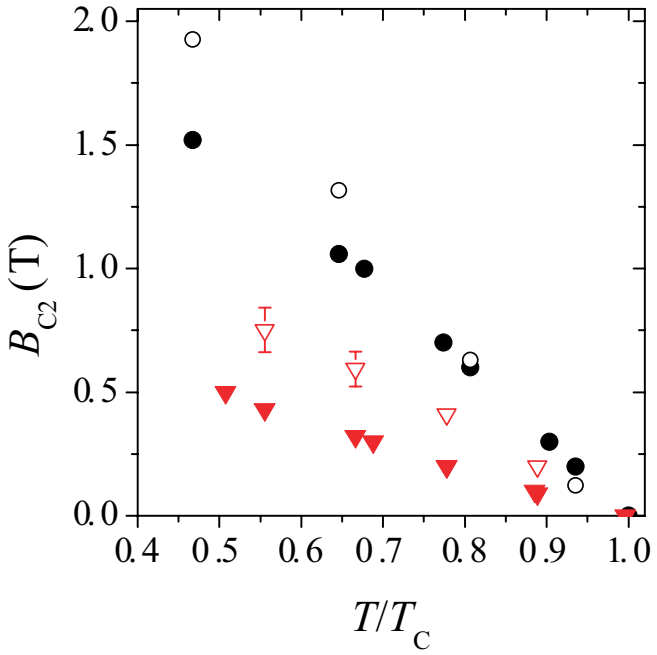

FIG. 7. (Color online) Upper critical field B_{c2} of the 10-nm film obtained by the 90% criterion from the microwave absorption measurements (black full circles). Upper critical field B_{c2}^{*} of the same sample obtained from the linear section of b (black opened circles). The same is shown for the 40-nm film by red triangles.

rameter due to the overlapping of vortices in higher fields is one of the reasons. The other reason for further suppression of the actual B_{c2} value can be found in spin paramagnetic effects and spin-orbit scattering.[38] This effect is not significant in our niobium samples since the upper critical fields are low enough, but in HTSCs, one can expect significant suppression of B_{c2} in the fields of the order of 100 T. As a consequence, the transition to the normal state is due to a combination of effects, and could not be related uniquely to the coherence length. However, the microwave determination of flow resistance in low-field region gives the best estimate of the coherence length.

The comparison of B_{c2} and B_{c2}^{*} for the 40-nm film is also shown in Fig. 7. The B_{c2}^{*} values are significantly higher than B_{c2}, but one should take this result with caution since there is no strictly linear part of b field dependence. This is not surprising since $\kappa \approx 1.5$ does not meet a high-κ condition needed for B_{c2}^{*} extraction.

VI. CONCLUSIONS

We have measured temperature and magnetic-field dependence of the microwave response of high quality niobium films in a perpendicular static magnetic field. The data have been analyzed by the effective conductivity model for the high-κ type-II superconductors in the mixed state. Our analysis shows that this model yields consistent results when applied in fields not too close to the transition to the normal state. Thin niobium films show strong pinning probably due to the surface pinning centers. The depinning frequency for the 10-nm film is $\nu_0 \approx 20$ GHz, and for the 40-nm film it is $\nu_0 \approx 7$ GHz. In thicker samples the depinning frequency is lower than 1 GHz. One should measure both the microwave absorption and the frequency shift in order to determine flow resistivity for samples with high values of depinning frequency, as usually found in HTSCs.

Although the bulk niobium samples have a GL parameter κ of the order of unity, very thin niobium films have higher κ values. They can serve as a model system for the upper critical field determination of high-κ superconducting samples. In HTSCs generally, upper critical fields are of the order of hundreds of T, and they are unreachable by laboratory magnets. Conventional methods for the determination of B_{c2} (transport measurements, susceptibility, torque, etc.) are based on the crossover to the normal state when the applied field equals B_{c2}. The determination of upper critical field is therefore reduced to a narrow temperature region close to T_c. The values for lower temperatures are usually determined by an extrapolation. The correctness of such extrapolations depends on the model used and there is no assurance that it holds also in HTSCs. On the other hand, pulsed methods used to reach high applied fields [up to 400 T (Ref. 39)] are nonequilibrium methods and very sensitive to induction, critical currents, etc. In this paper microwave response was measured up to the upper critical field which is for niobium samples reachable by conventional magnets. The upper critical fields are determined by the flow resistivity in low fields (B_{c2}^{*}) and by the crossover to the normal state (B_{c2}). The two methods give slightly different results. The B_{c2} defined as the crossover field to the normal state has certainly great technological importance. However, at high fields, typical for HTSCs, paramagnetic effects induce depairing and reduce order parameter. If one calculates the coherence lengths from B_{c2} values obtained in this way, the values are overestimated. For the considerations of the physical parameters of the superconducting state, it is better to determine the coherence length in rather low magnetic fields, deeply in the superconducting state. The microwave method tested here is certainly suitable for the determination of B_{c2}^{*} which gives correct values of effective vortex radii at a given temperature in the fields low enough that vortices do not overlap. Therefore the method is relevant for the determination of coherence lengths, especially in HTSCs.

ACKNOWLEDGMENTS

We thank M. Basletić and E. Tafra for the help in the measurements of ρ_n.

*Electronic address: mpozek@phy.hr
†Present address: Agilent Technologies R&D and Marketing GmbH & Co. KG, Herrenberger Strasse 130, D-71034 Böblingen, Germany.

[1] R. E. Glover III and M. Tinkham, Phys. Rev. **108**, 243 (1957).
[2] M. A. Biondi and M. P. Garfunkel, Phys. Rev. **116**, 853 (1959).
[3] O. Klein, E. J. Nicol, K. Holczer, and G. Grüner, Phys. Rev. B **50**, 6307 (1994), and the historical overview there.
[4] M. Cardona, G. Fischer, and B. Rosenblum, Phys. Rev. Lett. **12**, 101 (1964).
[5] B. Rosenblum and M. Cardona, Phys. Rev. Lett. **12**, 657 (1964).
[6] J. I. Gittleman and B. Rosenblum, Phys. Rev. Lett. **16**, 734 (1966).
[7] W. N. Hardy, D. A. Bonn, D. C. Morgan, R. Liang, and K. Zhang, Phys. Rev. Lett. **70**, 3999 (1993).
[8] A. R. Strnad, C. F. Hempstead, and Y. B. Kim, Phys. Rev. Lett. **13**, 794 (1964).
[9] T. T. M. Palstra, B. Battlog, R. B. van Dover, L. F. Schneemeyer, and J. V. Waszczak, Phys. Rev. B **41**, 6621 (1990).
[10] W. Klein, R. P. Huebener, S. Gauss, and J. Parisi, J. Low Temp. Phys. **61**, 413 (1985).
[11] S. G. Doettinger, R. P. Huebener, R. Gerdemann, A. Kühle, S. Anders, T. G. Träuble, and J. C. Villegier, Phys. Rev. Lett. **73**, 1691 (1994).
[12] Z. L. Xiao and P. Ziemann, Phys. Rev. B **53**, 15265 (1996).
[13] B. J. Ruck, J. C. Abele, H. J. Trodahl, S. A. Brown, and P. Lynam, Phys. Rev. Lett. **78**, 3378 (1997).
[14] M. N. Kunchur, Phys. Rev. Lett. **89**, 137005 (2002).
[15] D. Babić, J. Bentner, C. Sürgers, and C. Strunk, Phys. Rev. B **69**, 092510 (2004).
[16] M. Golosovsky, M. Tsindlekht, H. Chayet, and D. Davidov, Phys. Rev. B **50**, 470 (1994); M. Golosovsky, M. Tsindlekht, and D. Davidov, Supercond. Sci. Technol. **9**, 1 (1996).
[17] M. W. Coffey and J. R. Clem, Phys. Rev. Lett. **67**, 386 (1991); Phys. Rev. B **46**, 11757 (1992).
[18] E. H. Brandt, Phys. Rev. Lett. **67**, 2219 (1991).
[19] A. Dulčić and M. Požek, Physica C **218**, 449 (1993); Fiz. A **2**, 43 (1993).
[20] J. Bardeen and M. J. Stephen, Phys. Rev. **140**, A1197 (1965).
[21] S. Bernath, T. Wagner, S. Hofmann, and M. Rühle, Surf. Sci. **400**, 335 (1998).
[22] M. Gao, C. Scheu, T. Wagner, W. Kurz, and M. Rühle, Z. Metallkd. **93**, 438 (2002).
[23] T. Wagner, J. Mater. Res. **13**, 693 (1998).
[24] S. A. Wolf, J. J. Kennedy, and M. Nisenoff, J. Vac. Sci. Technol. **13**, 145 (1976).
[25] J. Kodama, M. Itoh, and H. Hirai, J. Appl. Phys. **54**, 4050 (1983).
[26] M. S. M. Minhaj, S. Meepagala, J. T. Chen, and L. E. Wenger, Phys. Rev. B **49**, 15235 (1994).
[27] S. I. Park and T. H. Geballe, Physica B & C **135**, 108 (1986).
[28] A. I. Gubin, K. S. Il'in, S. A. Vitusevich, M. Siegel, and N. Klein, Phys. Rev. B **72**, 064503 (2005).
[29] J. W. P. Hsu and A. Kapitulnik, Phys. Rev. B **45**, 4819 (1992).
[30] Leon N. Cooper, Phys. Rev. Lett. **6**, 689 (1961).
[31] R. Blaschke and R. Blocksdorf, Z. Phys. B: Condens. Matter **49**, 99 (1982).
[32] B. Nebendahl, D.-N. Peligrad, M. Požek, A. Dulčić, and M. Mehring, Rev. Sci. Instrum. **72**, 1876 (2001).
[33] D.-N. Peligrad, B. Nebendahl, M. Mehring, A. Dulčić, M. Požek, and D. Paar, Phys. Rev. B **64**, 224504 (2001).
[34] M. Tinkham, *Introduction to Superconductivity* (McGraw-Hill, New York, 1996).
[35] D.-N. Peligrad, B. Nebendahl, C. Kessler, M. Mehring, A. Dulčić, M. Požek, and D. Paar, Phys. Rev. B **58**, 11652 (1998).
[36] For numerical determination of b and ω_0 we have used the FindRoot routine of the commercial software MATHEMATICA (Wolfram Research).
[37] A. I. Larkin and Y. N. Ovchinnikov, in *Nonequilibrium Superconductivity*, edited by D. N. Lengenberg and A. I. Larkin (North-Holland, Amsterdam, 1986), p. 493.
[38] N. R. Werthamer, E. Helfand, and P. C. Hohenberg, Phys. Rev. **147**, 295 (1966).
[39] T. Sekitani, N. Miura, S. Ikeda, Y. H. Matsuda, and Y. Shiohara, Physica B **346-347**, 295 (2004).